RNA (1998), *4*:1124–1133. Cambridge University Press. Printed in the USA.

Characterization of an anti-RNA recombinant autoantibody fragment (scFv) isolated from a phage display library and detailed analysis of its binding site on U1 snRNA

S.W.M. TEUNISSEN, M.H.W. STASSEN, G.J.M. PRUIJN, W.J. VAN VENROOIJ, and R.M.A. HOET[1]

Department of Biochemistry, University of Nijmegen, 6500 HB Nijmegen, The Netherlands

ABSTRACT

This is the first study in which the complex of a monoclonal autoantibody fragment and its target, stem loop II of U1 snRNA, was investigated with enzymatic and chemical probing. A phage display antibody library derived from bone marrow cells of an SLE patient was used for selection of scFvs specific for stem loop II. The scFv specificity was tested by RNA immunoprecipitation and nitrocellulose filter binding competition experiments. Immunofluorescence data and immunoprecipitation of U1 snRNPs containing U1A protein, pointed to an scFv binding site different from the U1A binding site. The scFv binding site on stem loop II was determined by footprinting experiments using RNase A, RNase V1, and hydroxyl radicals. The results show that the binding site covers three sequence elements on the RNA, one on the 5′ strand of the stem and two on the 3′ strand. Hypersensitivity of three loop nucleotides suggests a conformational change of the RNA upon antibody binding. A three-dimensional representation of stem loop II reveals a juxtapositioning of the three protected regions on one side of the helix, spanning approximately one helical turn. The location of the scFv binding site on stem loop II is in full agreement with the finding that both the U1A protein and the scFv are able to bind stem loop II simultaneously. As a consequence, this recombinant monoclonal anti-U1 snRNA scFv might be very useful in studies on U1 snRNPs and its involvement in cellular processes like splicing.

Keywords: footprinting; phage display; RNA–antibody complex; single-chain variable fragment; U1 snRNA

INTRODUCTION

Patients suffering from autoimmune diseases produce antibodies directed to a variety of intracellular self-antigens. In patients with systemic lupus erythematosus (SLE), antibodies recognizing the U1 small nuclear ribonucleoprotein particle (snRNP) are often found. U1 snRNP consists of an RNA molecule (U1 snRNA) bound by several proteins and plays an important role in splicing of pre-mRNA. Three proteins are specifically associated with U1 snRNP: U1A, U1C, and the U1-70K protein. The remaining U1 snRNP proteins (Sm proteins) are also associated with other snRNPs (for a review, see Klein Gunnewiek et al., 1997).

The sera of SLE patients may not only contain antibodies directed against the protein components of the U1 snRNP, but also antibodies directed against the U1 snRNA itself (Van Venrooij et al., 1990). Previous studies have shown that the main targets of these autoantibodies are stem loops II and IV of U1 snRNA. Hoet et al. (1992) utilized mutant RNAs to study these epitopes on the U1 snRNA, whereas Tsai and Keene (1993) and St. Clair and Burch (1996) employed an RNA epitope library. Both anti-U1 snRNA antibody populations (anti-stem loop II and anti-stem loop IV) have been purified and were able to precipitate the native U1 snRNP, indicating that the antigenic regions are accessible (Hoet et al., 1993). Stem loop II and, in particular, the loop of this structural element is involved in the binding of the U1A protein (Lutz-Freyermuth & Keene, 1989; Patton et al., 1989; Sherly et al., 1989; Surowy et al., 1989; Bach et al., 1990; Jessen et al., 1991). A protein interacting with stem loop IV has not yet been described.

Both human and murine monoclonal antibodies directed to U1 snRNP protein components are available for studying the U1 snRNP particle (Billings et al., 1982;

Reprint requests to: S.W.M. Teunissen, Department of Biochemistry, University of Nijmegen, P.O. Box 9101, 6500 HB Nijmegen, The Netherlands; e-mail: s.teunissen@bioch.kun.nl.

[1]Present address: Department of Pathology, University Hospital Maastricht, P.O. Box 5800, 6202 AZ Maastricht, The Netherlands.

Habets et al., 1989; De Wildt et al., 1996). Monoclonal antibodies against the U1 snRNA are not available yet. Thus far, only affinity-purified antibodies or in situ hybridization of modified antisense probes could be used to study the U1 snRNP via its RNA molecule (Carmo-Fonseca et al., 1991; Hoet et al., 1993). Therefore, we set out to produce an anti-U1 snRNA monoclonal antibody. For this purpose, a phage display antibody library was prepared from an anti-U1 snRNA positive SLE patient and used subsequently to select anti-U1 snRNA antibodies. These selections resulted in the isolation of two single-chain variable fragments (scFv) specific for stem loop II of U1 snRNA. Like the patients' antibodies, the selected scFvs were able to bind intact U1 snRNPs. One of the scFvs was further characterized in detail. The scFv binding region on U1 snRNA was determined by footprinting analyses using RNase A, RNase V1, and Fe(II)EDTA. Finally, the scFv binding site was visualized in a three-dimensional model of stem loop II RNA.

RESULTS

Selection of U1 snRNA specific scFvs

A phage display antibody library was prepared from SLE patient Z5 whose serum contained antibodies directed against U1 snRNA (Fig. 1A), more specifically anti-stem loop II and anti-stem loop IV antibodies (Hoet et al., 1993). First, RNA was isolated from bone marrow lymphocytes. Subsequently, immunoglobulin cDNA was synthesized and amplified using RT-PCR to obtain a scFv phage display library (R.M.A. Hoet, J. Raats, R. De Wildt, H. Dumortier, S. Muller, F. Van Den Hoogen, & W.J. Van Venrooij, submitted). From this library, two scFvs against U1 snRNA, termed Z5scFv3 and Z5scFv7, were selected using procedures described previously (De Wildt et al., 1996). Soluble scFvs were produced as a periplasmic secretion product containing both a VSV-tag and a His-tag for purification and detection purposes.

The specificity of the scFvs was first established using RNA immunoprecipitation. Because previous studies had revealed that patient Z5 produced anti-U1 snRNA autoantibodies reactive with stem loop II and stem loop IV of U1 snRNA, the corresponding subfragments of U1 snRNA (see Fig. 1B) were used to determine the specificity of the isolated scFvs. ScFvs were incubated with a mixture of [^{32}P]-labeled RNAs, consisting of U1 snRNA, stem loop II, and stem loop IV subfragments, and Th RNA [the RNA component of RNase MRP (Lindahl & Zengel, 1996)] as a negative control. Both Z5scFv3 and Z5scFv7 were able to immunoprecipitate U1 snRNA and stem loop II, but not stem loop IV (Fig. 1C). The negative control, Th RNA, was not precipitated. These results show that both scFvs specifically recognize stem loop II of U1 snRNA. Nitrocellulose filter binding competition assays, using several RNAs and double-stranded DNA, confirmed the specificity of these scFvs for stem loop II (data not shown). Possible cross-reactivity of the scFvs was tested with U1 proteins U1A, U1C, U1-70K, and SmB/B′ (by western blotting and ELISAs) and with nuclear extracts of HeLa cells (by western blotting). No cross-reactivities were detected (data not shown).

Because both scFvs were reactive with stem loop II and the expression level of Z5scFv7 was (for unknown reasons) reproducibly low, Z5scFv3 was chosen for a more detailed characterization.

Characterization of Z5scFv3

To determine which part of stem loop II is recognized, the binding of Z5scFv3 to two mutants of stem loop II was analyzed by immunoprecipitation. In mutant stem loop II^{ML}, four loop nucleotides, which are part of the U1A binding sequence (65-AUUG-69), were replaced by UGAU (stem loop II^{ML}, mutated loop; Fig. 1D). As can be seen in Figure 1D (lane 3), Z5scFv3 was able to precipitate stem loop II^{ML}. In the second mutant, the stem of stem loop II is replaced by stem IV of U2 snRNA (stem loop II^{MS}, mutated stem; Fig. 1E). In this case, Z5scFv3 failed to precipitate the RNA (Fig. 1E, lane 3). Taken together, these results indicate that Z5scFv3 specifically binds to the stem structure of stem loop II of U1 snRNA.

Next it was tested whether the Z5scFv3 was able to recognize its epitope in intact U1 snRNPs. First, a co-immunoprecipitation experiment was performed. The scFv was incubated with a ^{35}S-methionine-labeled cell extract and the co-immunoprecipitated proteins were analyzed by SDS-PAGE followed by autoradiography. As a positive control, anti-Sm antibodies were used (Fig. 1F, lane 2). Both types of antibodies were able to precipitate the U1 snRNP complex, visualized by the presence of the U1A and U1C proteins as well as the SmB/B′ and SmD proteins (see Fig. 1F, lanes 2 and 3). In a second type of experiment, the immunofluorescent staining pattern for the scFv in HEp-2 cells was determined. As can be seen in Figure 2, Z5scFv3 resulted in either a coiled body staining pattern or in a combined coiled body/nucleoplasmic speckled pattern very similar to that obtained with anti-U1A monoclonal antibody 9A9. Also Z5scFv7 resulted in staining of the coiled bodies. The appearance of nucleoplasmic speckles in addition to coiled bodies appeared to be dependent on the concentration of the antibody fragment. Similar observations have been made before with other anti-snRNP antibodies and with anti-U1C scFvs (R.M.A. Hoet, J. Raats, R. De Wildt, H. Dumortier, S. Muller, F. Van Den Hoogen, & W.J. Van Venrooij, submitted). The staining of both nucleoplasm and coiled bodies was sensitive to RNase activity (results not shown). Because Z5scFv3 is specific

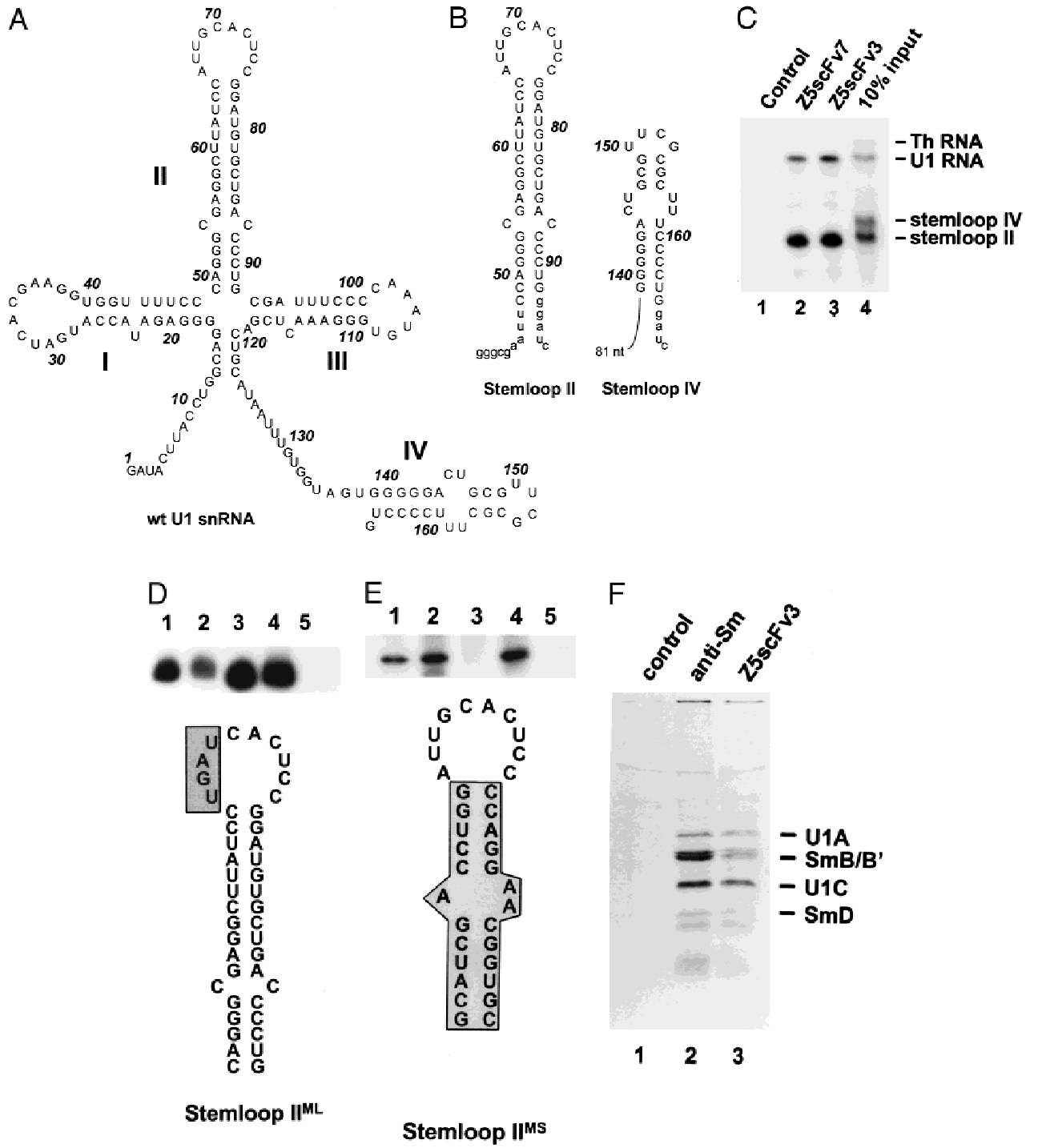

FIGURE 1. **A:** Human U1 snRNA in its proposed secondary structure according to Krol et al. (1990). Stem loop structures I–IV are indicated. **B:** Stem loop subfragments of U1 snRNA. Stem loop II (left) and stem loop IV (right) are shown. Vector-derived nucleotides are indicated in lower case. Numbering of the nucleotides is according to U1 snRNA. **C:** Immunoprecipitation of U1 snRNA, stem loop II, stem loop IV, and Th RNA. The stem loop II subfragment used in this experiment contains 45 extra vector-derived nucleotides, resulting in an RNA molecule of 89 nucleotides. Lane 1, control incubation with anti-VSV tag antibodies coupled to protein A beads via rabbit anti-mouse antibodies; lanes 2 and 3, RNAs precipitated by Z5scFv7 and Z5scFv3, respectively; lane 4, 10% of the RNA input. **D:** Immunoprecipitation of mutant stem loop II RNA. The mutant stem loop II^{ML} (Hoet et al., 1992) contains a mutated U1A binding sequence, replacing 65-AUUG-69 with UGAU (depicted by a shaded box). Lane 1, the input; lanes 2 and 3, supernatant and precipitated RNA by Z5scFv3, respectively; lanes 4 and 5, supernatant after immunoprecipitation and precipitated RNA of the control incubation with anti-VSV tag antibodies coupled to protein A beads via rabbit anti-mouse antibodies. **E:** Immunoprecipitation of mutant stem loop II RNA. In this mutant, stem II is changed into the stem of stem loop IV of U2 RNA (depicted by a shaded box), creating mutant stem loop II^{MS} (Hoet et al., 1992). Lane 1, the input; lanes 2 and 3, supernatant and precipitated RNA by Z5scFv3, respectively; lanes 4 and 5, supernatant after immunoprecipitation and precipitated RNA of the control incubation with anti-VSV tag antibodies coupled to protein A beads via rabbit anti-mouse antibodies. **F:** Precipitation of intact U1 snRNPs by Z5scFv3. U1 snRNP particles containing ^{35}S-labeled proteins were immunoprecipitated from a whole-cell extract using Z5scFv3 (lane 3), anti-Sm antibodies (lane 2), and a nonrelated antibody as negative control (lane 1).

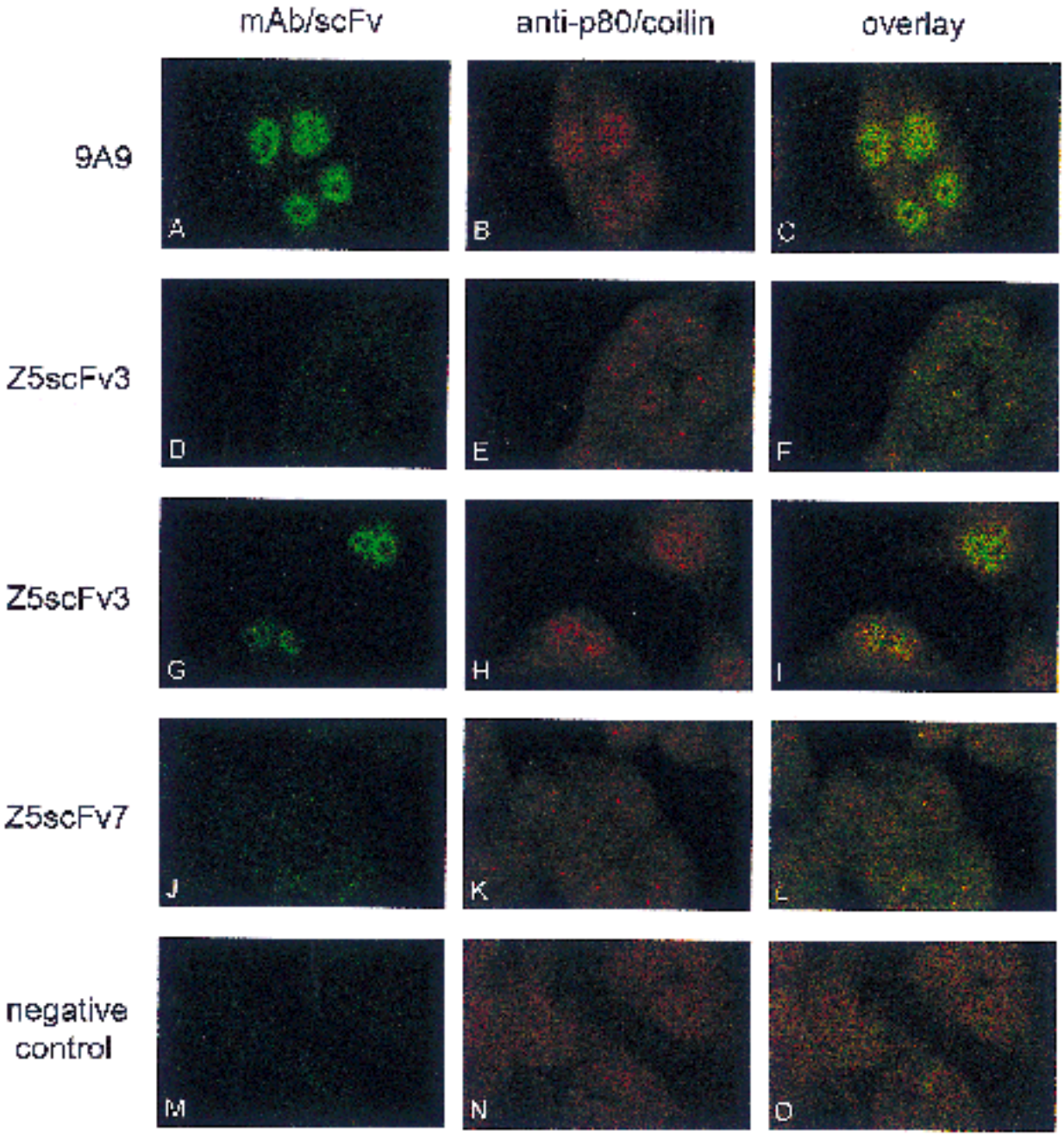

FIGURE 2. Anti-stem loop II antibodies stain coiled bodies and nucleoplasmic speckles. Immunofluorescent staining of HEp-2 cells with 9A9 (**A**, as a positive control), Z5scFv3 (**D** and **G**), Z5scFv7 (**J**), all showing green fluorescent patterns (denoted mAb/scFv), and anti-p80/coilin (**B**, **E**, **H**, and **K**, for co-localization studies) showing red fluorescence. Panels **C**, **F**, **I**, **L**, and **O** show the overlay of the two different antibody stainings, in which co-localization results in a yellow color. HEp-2 cells were incubated with antibody (in G–I, a five-fold higher concentration of Z5scFv3 was used, compared to D–F) and stained subsequently with anti-VSV-G (Boehringer Mannheim) and TexasRed conjugated rabbit-anti mouse Ig (Dako). As a negative control, the incubation with mAb/scFv and anti-p80/coilin was omitted (M–O).

for stem loop II of U1 snRNA, this result again suggests that the region of stem loop II that is recognized by the scFv is different from the region that is bound by the U1A protein. From these experiments, we conclude that both U1A and the Z5scFv3 autoantibody fragment are able to bind simultaneously to stem loop II of U1 snRNA.

Probing of the U1 snRNA–Z5scFv3 complex

For a more detailed characterization of the binding site of the patient-derived scFv, stem loop II of U1 snRNA (Fig. 1B) was probed with both enzymatic and chemical reagents in the presence and the absence of Z5scFv3. The scFv was first bound to beads and

allowed to bind to stem loop II. The bound stem loop II was subsequently probed with RNase A, RNase V1, or Fe(II)EDTA-generated hydroxyl radicals.

Enzymatic footprinting

Three regions on the RNA were found inaccessible to RNase V1 (cleaves phosphodiester bonds in double-stranded RNA) upon binding of the scFv, as can be seen in the experiment shown in Figure 3A (compare lanes 2–4 with lanes 6–8). The first region extends from G53 to U61 (nucleotide numbering as in Fig. 1B), covering a large central portion of the stem. The other regions, G77–G82 and G92–G93, are located on the opposite strand of the RNA (Fig. 3A), although it should be noted that the interpretation for G93 was obscured by spontaneous RNA breaks in some experiments. These results, however, confirm that the binding site of the scFv is different from the U1A binding site. No data were obtained for the region G83–G91, because RNase V1 did not cleave the free nor the complexed RNA at these positions. The probing results for the free RNA molecule are in complete agreement with the RNase V1 probing data for U1 snRNA described by Krol et al. (1990). The data are summarized in Figure 4A.

An unexpected observation was the increased sensitivity to RNase V1 of the bonds 3′ of C73–C75 in the RNA–scFv complex (see Fig. 3A, lanes 3 and 4, and Fig. 4A). This suggests that binding of the scFv induces stacking of the bases of the last three loop nucleotides, making them susceptible to RNase V1 cleavage. This could be the result of a more general stabilization of the helix structure, suggesting that the binding of Z5scFv3 to stem loop II induces some structural changes in the RNA.

Probing with RNase A (cleaves 3′ of single-stranded pyrimidines) did not show a protection pattern. The enzyme was able to cleave the same bonds in both the RNA–scFv complex and the free RNA, i.e., those in the loop of the RNA (nt 66–74), which is in agreement with the data described above suggesting that the scFv binds to the stem region on stem loop II (data not shown).

Chemical footprinting

Because ribonucleases are relatively large molecules, the protected regions might appear larger due to steric hindrance. We therefore used hydroxyl radicals generated by Fe(II)EDTA to obtain more detailed information on the accessibility of the riboses. An example of such a Fe(II)EDTA probing experiment is shown in Figure 3B. Lanes 1 and 3 represent control incubations in the absence of Fe(II)EDTA. A comparison of lanes 2 and 4 reveals three regions in stem loop II that are protected by the bound scFv against hydroxyl radical-induced cleavage. The combined phosphorimaging data of Fe(II)EDTA experiments were used to calculate a percentage protection of each nucleotide (upper panel of Fig. 4B). These data delineate the binding region of Z5scFv3 found by RNase V1 to nt C54–G58 on the 5′ strand of the stem and to G77–U80 and C87–C88 on the 3′ strand of the stem (lower panel of Fig. 4B).

If the Z5scFv3 binding site is highlighted in the three-dimensional model of the stem (Krol et al., 1990), all protected nucleotides appear to reside on the same side of the stem. The binding site encompasses three juxtaposed sequence elements on the helix (nt 54–58, nt 77–80, and nt 87–88). This is shown as stereo views from two different angles (Fig. 5A,B), with the Z5scFv3 binding site highlighted in red. The loop II structure of U1 snRNA, as determined by X-ray crystallography (Oubridge et al., 1994), is incorporated in the model (shown in yellow) together with the first RNA-binding domain of U1A protein (represented as a green shaded ribbon). This model shows that the Z5scFv3 binding site is spatially separated from the U1A binding site and is located at the other side of the RNA molecule (with respect to the helix axis). This model further suggests that both the U1A protein and Z5scFv3 are able to bind the RNA simultaneously.

DISCUSSION

In this study, human monoclonal autoantibodies directed to an RNA molecule have been described. Their specificity for U1 snRNA, in particular stem loop II of U1 snRNA, was established by immunoprecipitation and by nitrocellulose binding competition assays. One of these human monoclonal antibodies (Z5scFv3) was characterized in more detail. It binds specifically to the stem of the U1 snRNA stem loop II, suggesting that the scFv recognizes a structure distinct from the U1A binding site, which is known to bind the loop of stem loop II (Lutz-Freyermuth & Keene, 1989; Patton et al., 1989; Sherly et al., 1989; Surowy et al., 1989; Bach et al., 1990; Jessen et al., 1991). The simultaneous binding of Z5scFv3 and U1A to U1 snRNA was substantiated by immunofluorescence data and by the ability of the autoantibody fragment to precipitate U1A containing U1 snRNPs from a total cell extract. The present data, however, do not provide information about the possible difference in affinity of the scFv toward either the intact U1 snRNP or the naked U1 snRNA. Nevertheless, the binding of U1 snRNP in both immunoprecipitation and immunofluorescence imply that this scFv might be an attractive tool for biochemical and cell biological studies on U1 snRNP. In view of its specificity, it provides an alternative to U1 snRNA-specific antisense oligonucleotide probes (Carmo-Fonseca et al., 1991). For some applications, it may even be superior to antisense oligonucleotides, because the latter probes are directed preferentially to single-stranded regions in the RNA that, in general, coincide with functionally important

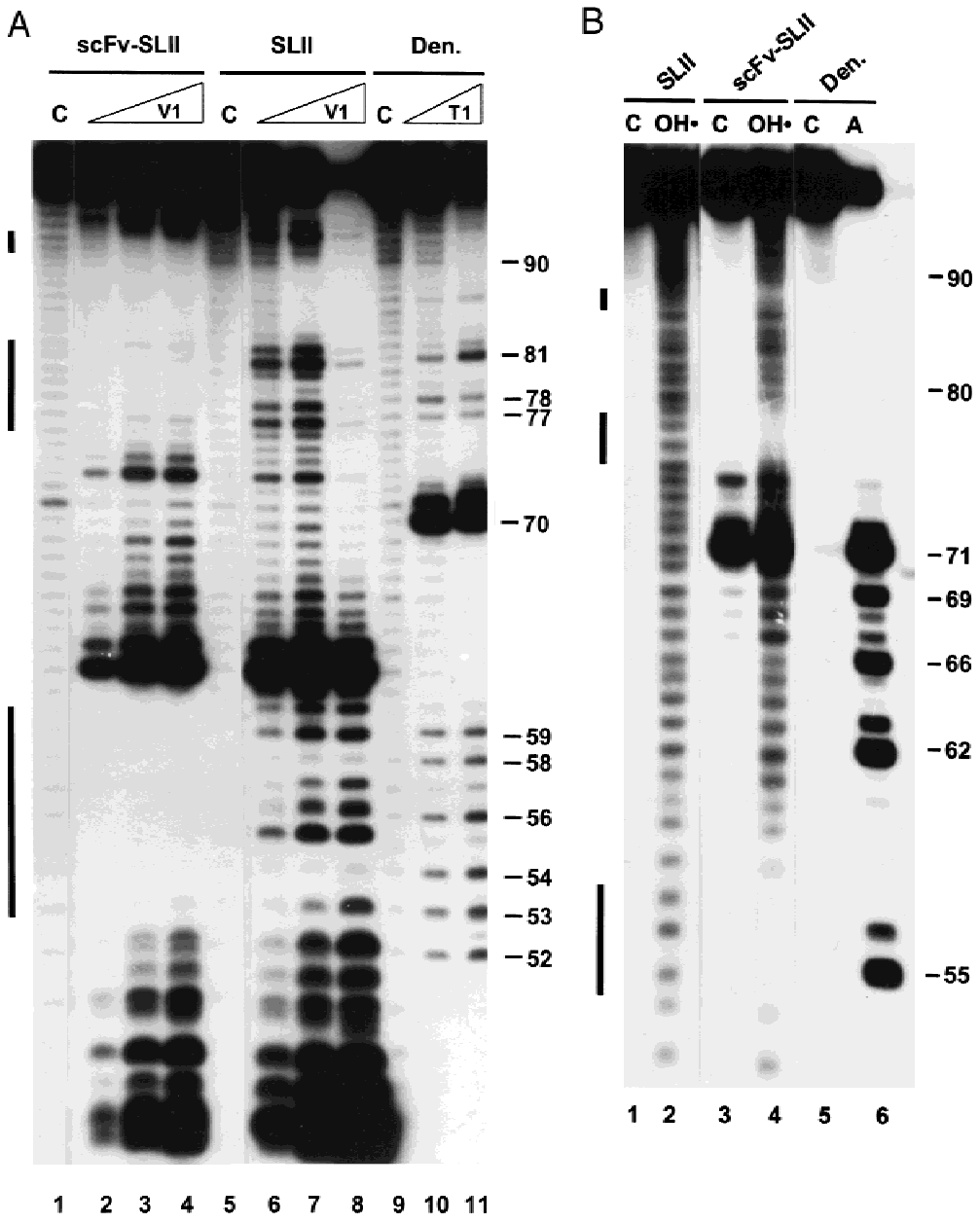

FIGURE 3. Footprint analysis of the Z5scFv3–stem loop II complex. **A:** Probing experiment using the double-stranded RNA specific RNase V1. Both the free and the complexed RNA were subjected to RNase V1 degradation. Lanes 1, 5, and 9, control incubations in which the RNase was omitted. The Z5scFv3–stem loop II complex is probed in lanes 2–4 (denoted scFv-SLII), with increasing amounts of RNase V1. Free RNA is probed with increasing amounts of RNase V1 in lanes 6–8 (denoted SLII). Cleavage positions were deduced from sequence ladders of RNase T1 (lanes 10 and 11). The cleavage product of RNase V1 migrates faster than the corresponding RNase T1 cleavage product, resulting in a difference of one nucleotide. Nucleotide positions indicated on the right are numbered according to the RNase V1 cleavages. Solid lines at the left indicate regions in the RNA that are protected by Z5scFv3. **B:** Probing experiment using Fe(II)EDTA. Lanes 1 and 2, probing of the free RNA (denoted SLII); lanes 3 and 4, probing of the Z5scFv3–stem loop II complex (denoted scFv-SLII); lanes 5 and 6, sequence ladder of the free RNA obtained under denaturing conditions using RNase A. Lanes 1, 3, and 5 are control incubations in which the reagent was omitted. Cleavage positions were deduced from the sequence ladder of RNase A (lane 6). The labeled product from cleavage by hydroxyl radicals has an additional phosphate group. The migration therefore differs by one nucleotide from the RNase A sequence ladder. Nucleotide positions indicated on the right are numbered according to the hydroxyl radical cleavages. Solid lines at the left indicate regions in the RNA that are protected by Z5scFv3.

elements, like the 5′-end of U1 snRNA, which is involved in 5′-splice-site recognition, and loop sequences, which are important for protein binding (reviewed in Klein Gunnewiek et al., 1997). Because no (major) structural changes in the RNA seem to be required for recognition of U1 snRNA by the scFv, and because no specialized and laborious techniques are required to visualize U1 snRNA with the scFv,

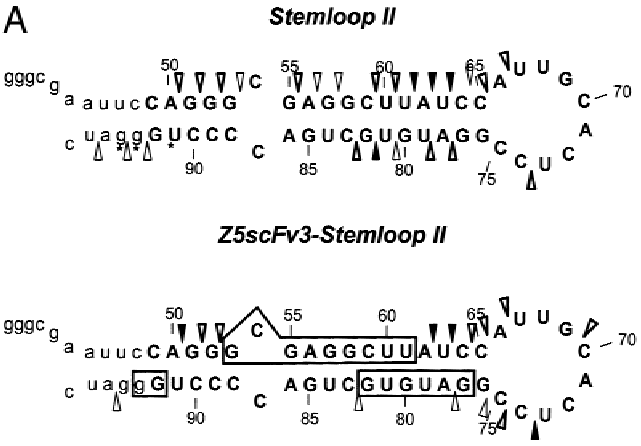

FIGURE 4. Summary of footprinting data. **A:** Summary of probing data of RNase V1 cleavages. Enzymatic cleavages are indicated by open triangles (weak), open bold triangles (normal), and solid triangles (strong). RNA breaks that occurred in the control incubations are indicated with asterisks. Protected regions are indicated by boxes. Vector-derived nucleotides are indicated in lower case. **B:** Summary of Fe(II)EDTA probing data. Upper panel shows the average protection for each nucleotide, calculated from phosphorimaging data. Protected regions above 30% protection are boxed in the lower panel. It should be noted that the data for nt 67–75 were obscured by natural RNA breaks in the control incubations.

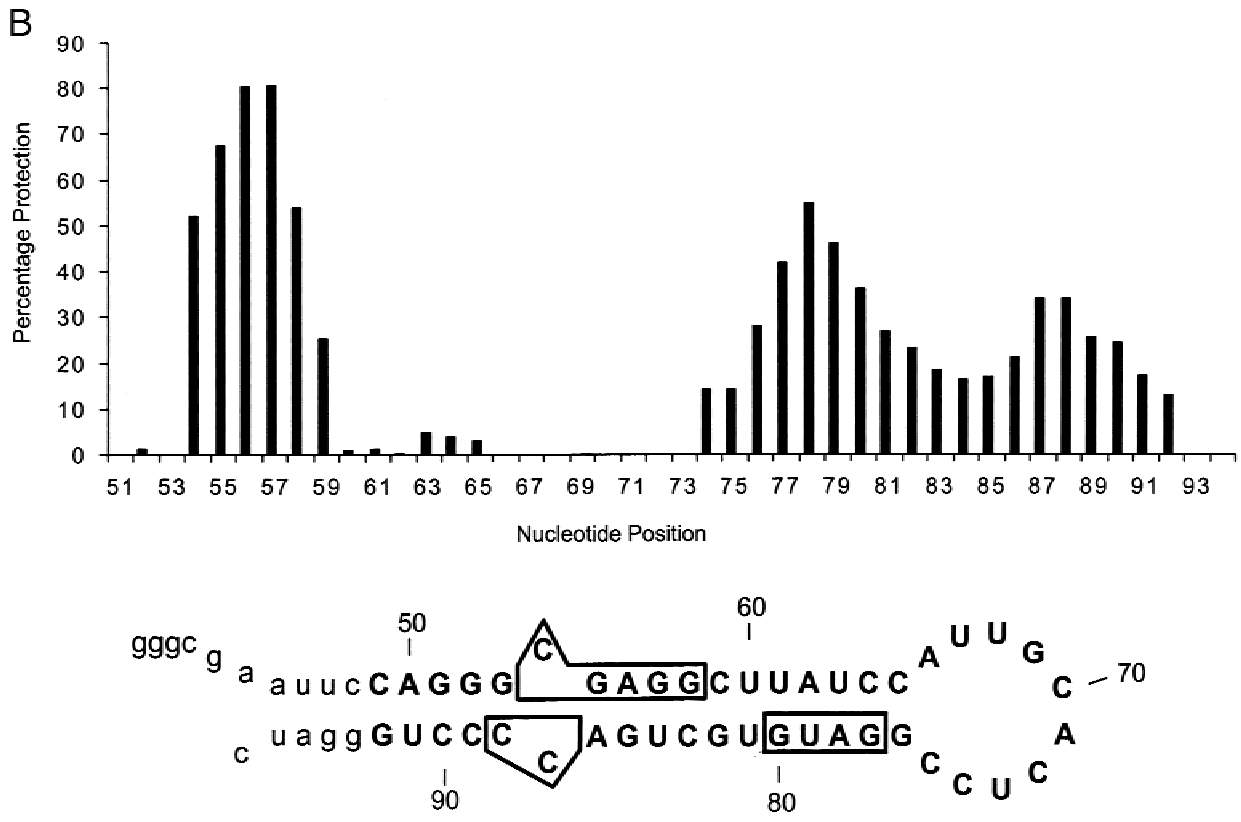

this recombinant antibody fragment provides an excellent reagent for cell biological studies on U1 snRNA. Moreover, because, in principle, any epitope tag can be introduced in the scFv (a VSV-G tag was used in our studies), these antibodies can be combined easily with conventional murine monoclonal antibodies in double staining experiments.

It should be noted that we still do not know whether the Z5scFv3 epitope is accessible in higher-order complexes like the spliceosome. Nevertheless, the immunofluorescence patterns obtained with the anti-U1 RNA scFvs indicated that the stem loop II epitope is accessible in both nucleoplasmic U1 RNA and U1 RNA localized in coiled bodies. At relatively low concentrations of scFvs, merely coiled body staining was evident, which is in agreement with previously published data indicating that the highest concentrations of splicing snRNPs are found in this subnuclear compartment, an organelle that has been proposed to be involved in some aspect of snRNP maturation, transport, or recycling (Bohmann et al., 1995). The anti-U1 RNA scFv staining pattern is similar to those reported previously for anti-U1 snRNP-specific antibodies (Habets et al., 1989; Klein Gunnewiek & Van Venrooij, 1994) and to the pattern obtained by in situ hybridization with U1 snRNA-specific probes. Most interestingly, based upon the results of the latter type of experiments, it has been suggested that the relative concentration of U1 snRNA in coiled

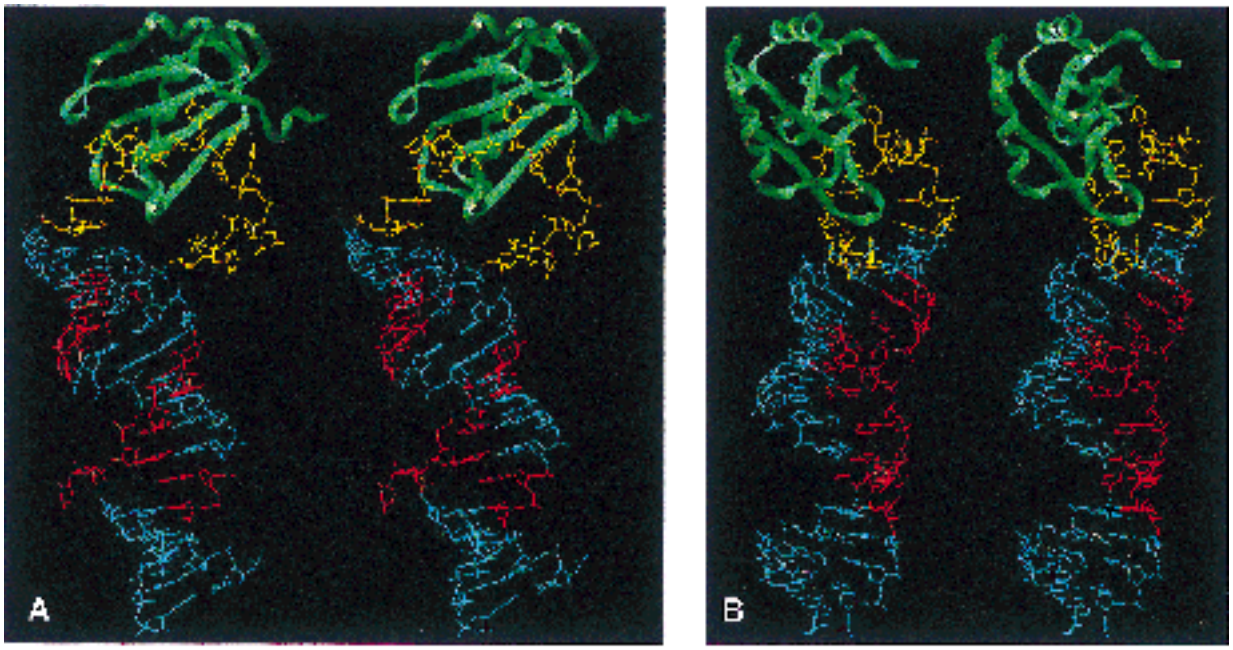

FIGURE 5. Stereo view of the binding site of Z5scFv3 on stem loop II. Front view (**A**) and side view (**B**) of stem loop II [reconstructed from the crystal structure of the U1A binding site (Oubridge et al., 1994) and the proposed three-dimensional model of stem loop II (Krol et al., 1990)]. U1A binding sequence on the RNA is indicated in yellow. Protected regions on stem loop II are shown in red. RNA-binding domain of the U1A protein in association with the loop is shown as a green shaded ribbon.

bodies might be lower than that of the other splicing snRNAs (Carmo-Fonseca et al., 1991, 1992; Matera & Ward, 1993). The present scFv data also suggest that U1 snRNA accumulates in the coiled bodies in HEp-2 cells. The discrepancy with the in situ hybridization data might be explained (in part) by the potentially reduced accessibility of U1 snRNA sequences complementary to the in situ hybridization probes in coiled bodies.

The RNase V1 structure probing data of U1 snRNA stem loop II are in complete agreement with previously published results obtained with complete U1 snRNA (Krol et al., 1990). These data and the immunoprecipitation of stem loop II indicate that the vector-derived nucleotides did not (markedly) influence the formation of the proposed stem loop structure. Our RNase V1 probing data do suggest that the stem structure is lengthened somewhat by base pairing of some of these vector-derived nucleotides (see Fig. 4A). A comparison of the RNase V1 cleavages in the free RNA with cleavages in the scFv–RNA complex indicated three protected regions in the complex. One region is located in the 5′ part of the stem of stem loop II, and two regions in the 3′ part. A reduced efficiency of a particular cleavage is not necessarily the result of steric hindrance due to the binding of the scFv. It could also result from a structural change, i.e., from double-stranded to single-stranded RNA. However, the RNase A probing of the scFv–RNA complex did not show additional cleavage sites in regions that are double-stranded in the free RNA, thus arguing against such a possibility. Because of the size of nucleases, footprints found by RNases usually are larger than the region actually involved in the interaction with protein.

A more refined protection pattern, nicely correlating with the RNase V1 data, was obtained with hydroxyl radicals (Fig. 4B). It should be noted that the Z5scFv3 binding region contains some unusual base pairs: C54–C87, G55–A86, and A56–G85. Because such base pairs distort the normal helical (A-form) structure of an RNA, they might be very important for the specific recognition of the RNA by the scFv. An interesting possibility would be that the major groove, which is deep and narrow in an A-form helix and therefore inaccessible for protein side chains, is widened to some extent by the presence of these unusual base pairs. Specificity is more easily achieved by interactions in the major groove in comparison with minor groove contacts, in particular in the case of A-U base pairs. Because the center of the epitope recognized by Z5scFv3 coincides with the unusual base pairs (positions 54–58), it is tempting to speculate that the specificity of the antibody fragment is determined by hydrogen bonds and specific electrostatic interactions in this unique (distorted) helical region in stem loop II of U1 snRNA. Structural data, obtained by, for instance, X-ray diffraction of co-crystals, are required to shed more light on this.

To obtain a more three-dimensional impression of the Z5scFv3 epitope structure, a model for U1 snRNA stem loop II was built, based upon literature data for stem (Krol et al., 1990) and loop structure (Oubridge

et al., 1994). A projection of sequence elements protected by Z5scFv3 on this three-dimensional representation of U1 snRNA stem loop II revealed that these elements are juxtaposed on one side of the helix and that the complete epitope covers approximately one helical turn. Strikingly, in this structural model, the U1A protein recognition site, which has been well defined by many experimental data (Lutz-Freyermuth & Keene, 1989; Patton et al., 1989; Sherly et al., 1989; Surowy et al., 1989; Bach et al., 1990; Jessen et al., 1991; Oubridge et al., 1994), is not only spatially separated from the Z5scFv3 epitope through its location in the loop, but also appears to be positioned on the opposite side (with respect to the helix axis) of the RNA molecule. Accordingly, it is not surprising that U1A and Z5scFv3 are able to bind to stem loop II simultaneously.

An interesting aspect from an immunological point of view is the fact that Z5scFv3 was derived from a phage display library reflecting the antibody repertoire of an autoimmune patient. The observation that this autoantibody recognizes part of the stem structure of stem loop II, even in a completely assembled U1snRNP complex, is compatible with the idea that the intact U1snRNP complex, at some stage during the development of the autoimmune response, is the (auto)antigen exposed to the immune system.

MATERIALS AND METHODS

Preparation of RNA and production of the U1A protein

The full-length U1 snRNA, the stem loop II, and the stem loop IV subfragments (Fig. 1) are described by Hoet et al. (1992). The constructs for stem loop II and IV code for nt C49–G92 and G139–G165, respectively. After T7 transcription of the *Bam*H I digest, stem loop II contains 15 extra vector-derived nucleotides (see Fig. 1B) and 45 extra vector-derived nucleotides for the subfragment used in Figure 1C, whereas stem loop IV contains 86 extra vector-derived nucleotides (see Fig. 1B). The Th RNA construct was a kind gift of Dr. H. Pluk. Transcription and 5′-end-labeling of the RNA was performed essentially as described in Teunissen et al. (1997). To obtain ^{32}P-labeled RNA, in vitro transcription was performed in the presence of [α-^{32}P]UTP. Production and purification of recombinant U1A protein in *Escherichia coli* was performed as described previously (Boelens et al., 1993).

Selection and screening of scFvs

To obtain a scFv-producing library, RNA was isolated from bone marrow lymphocytes. Subsequently, cDNA was synthesized and amplified using PCR (R.M.A. Hoet, J. Raats, R. De Wildt, H. Dumortier, S. Muller, F. Van Den Hoogen, & W.J. Van Venrooij, submitted). The selection protocol followed was essentially as described in De Wildt et al. (1996), using immunotubes (Nunc, Maxisorp) coated with U1 snRNA to select scFvs. After three rounds of selection, scFv-clones were screened by a nitrocellulose filter binding assay.

^{35}S-labeled cell extract

HeLa (ATCC-CCL-2) monolayer cells were cultured in methionine-free medium for 1 h. Subsequently, the cells were incubated with 10 μCi/mL ^{35}S-methionine for 4 h at 37 °C, followed by an overnight incubation in complete medium. Cells were trypsinized and washed three times with cold PBS. After resuspension, the cells were subjected to three rounds of freeze-thawing, sonified, and centrifuged at 100,000 × *g*. Glycerol was added to the supernatant to a final percentage of 20%, which was subsequently stored at −70 °C until use.

Immunoprecipitations

A VSV-tagged scFv was coupled to 20 μL protein A agarose beads via rabbit anti-mouse immunoglobulins (Dako, 5 μL) and a mouse anti-VSV antibody (Boehringer Mannheim, 1667351; 0.5 mL supernatant) in 150 mM NaCl, 10 mM Tris-HCl, pH 7.5, and 0.05% NP-40 (De Wildt et al., 1996). In order to test the specificity of the antibodies, the immobilized scFvs were either incubated with a mixture of [^{32}P]-labeled RNAs (Th RNA, U1 snRNA, stem loop II, and stem loop IV) or with the [^{32}P]-labeled stem loop II^{ML} or stem loop II^{MS}. To determine whether Z5scFv3 was able to immunoprecipitate U1 snRNP complexes, the coupled antibody was incubated with ^{35}S-labeled cell extract. For probing reactions, the immobilized Z5scFv3 was incubated with stem loop II RNA at 4 °C in probing buffer: 100 mM KCl, 10 mM Tris-HCl, pH 7.5, 2.5 mM $MgCl_2$, 0.1% Tween-20, and 0.1% NP-40. The complexes were washed with probing buffer to remove unbound RNA, and subsequently subjected to probing agents.

Immunofluorescence staining of HEp-2 cells

Fixed HEp-2 (ATCC-CCL-23) cells were incubated with a periplasmic fraction of Z5scFv3 or Z5scFv7 (dialyzed against PBS) and bound antibody fragments were visualized by subsequent incubations with anti-VSV-G (Boehringer Mannheim) and FITC-conjugated goat anti-mouse Ig (Dako). Between each incubation step, the cells were washed briefly three times with PBS. The scFv was omitted in the negative control. The U1A specific monoclonal antibody 9A9 (Habets et al., 1989) was used as a positive control. For double-labeling experiments with anti-p80 coilin (rabbit serum R288, a kind gift of Dr. E. Chan), the cells were incubated with anti-p80 coilin (100-fold diluted in PBS) and Texas Red-conjugated donkey anti-rabbit Ig (Amersham) either prior to the scFv incubation or in combination with the scFv and the FITC-conjugated goat anti-mouse Ig, respectively. Confocal microscopy was used to obtain Z scans, which were superimposed for double stainings.

Probing reactions

Concentrations of enzymes and chemicals were optimized to obtain single hit conditions. Parallel incubations in which the probing agent was omitted were performed in order to detect spontaneous RNA breaks. RNase probing was performed essentially as described by Teunissen et al. (1997). Probing with Fe(II)EDTA was performed as described by Darsillo and

Huber (1991). In order to obtain single hit conditions, the concentrations of $Fe(II)SO_4$ (Aldrich), EDTA (Aldrich), ascorbic acid (Sigma), and H_2O_2 (Janssen Chimica) were varied, while maintaining a molar ratio of 1:2 for $Fe(II)SO_4$ and EDTA, respectively. Results were analyzed on a phosphorimager. The average percentage protection was calculated by subtracting the number of counts of the Z5scFv3–stem loop II complex from the number of counts of the naked RNA, after background correction, for each nucleotide position.

Construction of the three-dimensional RNA structural model

Structures were visualized on a Silicon Graphics Indy workstation with the SYBYL program (SYBYL Molecular Modeling Software, Version 6.3/6.4, Tripos Inc., St. Louis, Missouri). The model was constructed using PDB structure 1NRC for the loop (Oubridge et al., 1994) and the three-dimensional model proposed by Krol et al. (1990) for the stem structure. Base pairs of the stem from the crystal structure were fitted manually onto the corresponding base pairs of the model.

ACKNOWLEDGMENTS

Use of the services and facilities of the Dutch National NWO/SURF Expertise Center CAOS/CAMM, University of Nijmegen, The Netherlands, is gratefully acknowledged. Coordinates of the three-dimensional model of U1 snRNA were generously supplied by Dr. E. Westhof (I.M.B.C., CNRS, Strasbourg, France). We thank Y. van Aarssen and M. Pieffers for technical assistance and Dr. E. Chan (Scripps Research Institute, La Jolla, California) for the anti-p80 coilin antiserum. These investigations were supported by the Netherlands Foundation for Chemical Research (SON) with financial aid from the Netherlands Technology Foundation (STW grant 349-3026).

Received April 16, 1998; returned for revision May 14, 1998; revised manuscript received June 12, 1998

REFERENCES

Bach M, Krol A, Lührmann R. 1990. Structure-probing of U1 snRNPs gradually depleted of the U1-specific proteins A, C and 70k. Evidence that A interacts differentially with developmentally regulated mouse U1 snRNA variants. *Nucleic Acids Res 18*:449–457.

Billings PB, Allen RW, Jensen FC, Hoch SO. 1982. Anti-RNP monoclonal antibodies derived from a mouse strain with lupus-like autoimmunity. *J Immunol 128*:1176–1180.

Boelens WC, Jansen EJ, van Venrooij WJ, Stripecke R, Mattaj IW, Gunderson SI. 1993. The human U1 snRNP-specific U1A protein inhibits polyadenylation of its own pre-mRNA. *Cell 72*:881–892.

Bohmann K, Ferreira J, Santama N, Weis K, Lamond AI. 1995. Molecular analysis of the coiled body. *J Cell Sci 19*(suppl):107–113.

Carmo-Fonseca M, Pepperkok R, Carvalho MT, Lamond AI. 1992. Transcription-dependent colocalization of the U1, U2, U4/U6, and U5 snRNPs in coiled bodies. *J Cell Biol 117*:1–14.

Carmo-Fonseca M, Tollervey D, Pepperkok R, Barabino SML, Merdes A, Brunner C, Zamore PD, Green MR, Hurt W, Lamond AI. 1991. Mammalian nuclei contain foci which are highly enriched in components of the pre-mRNA splicing machinery. *EMBO J 10*:195–206.

Darsillo P, Huber PW. 1991. The use of chemical nucleases to analyze RNA–protein interactions. *J Biol Chem 266*:21075–21082.

De Wildt RMT, Finnern R, Ouwehand WH, Griffiths AD, Van Venrooij WJ, Hoet RMA. 1996. Characterization of human variable domain antibody fragments against the U1 RNA-associated A protein, selected from a synthetic and a patient-derived combinatorial V gene library. *Eur J Immunol 26*:629–639.

Habets WJ, Hoet MH, De Hong BAW, Van Der Kemp A, Van Venrooij WJ. 1989. Mapping of V cell epitopes on small nuclear ribonucleoproteins that react with human autoantibodies as well as with experimentally-induced mouse monoclonal antibodies. *J Immunol 143*:2560–2566.

Hoet RM, De Weerd P, Klein Gunnewiek J, Koornneef I, Van Venrooij WJ. 1992. Epitope regions on U1 small nuclear RNA recognized by anti-U1RNA-specific autoantibodies. *J Clin Invest 90*:1753–1762.

Hoet RM, Kastner B, Lührmann R, Van Venrooij WJ. 1993. Purification and characterization of human autoantibodies directed to specific regions on U1RNA; recognition of native U1RNP complexes. *Nucleic Acids Res 21*:5130–5136.

Jessen TH, Oubridge C, Teo CH, Pritchard C, Nagai K. 1991. Identification of molecular contacts between the U1 A small nuclear ribonucleoprotein and U1 RNA. *EMBO J 10*:3447–3456.

Klein Gunnewiek JMT, Van Venrooij WJ. 1994. Autoantigens contained in the U1 small nuclear ribonucleoprotein complex. In: Van Venrooij WJ, Maini RN, eds. *Manual of biological markers of disease*. Dordrecht: Kluwer Academic Publishers. pp B3.1:1–20.

Klein Gunnewiek JMT, Van De Putte LBA, Van Venrooij WJ. 1997. The U1 snRNP complex: An autoantigen in connective tissue diseases. An update. *Clin Exp Rheumatol 15*:549–560.

Krol A, Westhof E, Bach M, Lührmann R, Ebel JP, Carbon P. 1990. Solution structure of human U1 snRNA. Derivation of a possible three-dimensional model. *Nucleic Acids Res 18*:3803–3811.

Lindahl L, Zengel JM. 1996. RNase MRP and rRNA processing. *Mol Biol Rep 22*:69–73.

Lutz-Freyermuth C, Keene JD. 1989. The U1 RNA-binding site of the U1 small nuclear ribonucleoprotein (snRNP)-associated A protein suggests a similarity with U2 snRNPs. *Mol Cell Biol 9*:2975–2982.

Matera AG, Ward DC. 1993. Nucleoplasmic organization of small nuclear ribonucleoproteins in cultured human cells. *J Cell Biol 121*:715–727.

Oubridge C, Ito N, Evans PR, Teo CH, Nagai K. 1994. Crystal structure at 1.92 Å resolution of the ENA-binding domain of the U1A splicesomal protein complexed with an RNA hairpin. *Nature 372*:432–438.

Patton JR, Habets W, van Venrooij WJ, Pederson T. 1989. U1 small nuclear ribonucleoprotein particle-specific proteins interact with the first and second stem-loops of U1 RNA, with the A protein binding directly to the RNA independently of the 70K and Sm proteins. *Mol Cell Biol 9*:3360–3368.

Sherly D, Boelens W, van Venrooij WJ, Dathan NA, Hamm J, Mattaj IW. 1989. Identification of the RNA binding segment of human U1 A protein and definition of its binding site on U1 snRNA. *EMBO J 8*:4163–4170.

St. Clair EW, Burch JA Jr. 1996. In vitro RNA selection of an autoimmune epitope on stem-loop II of U1 RNA. *Clin Immunol Immunopathol 79*:60–70.

Surowy CS, van Santen VL, Scheib-Wixted SM, Spritz RA. 1989. Direct, sequence-specific binding of the human U1-70K ribonucleoprotein antigen protein to loop I of U1 small nuclear RNA. *Mol Cell Biol 9*:4179–4186.

Teunissen SWM, Van Gelder CWG, Van Venrooij WJ. 1997. Probing the 3′UTR structure of U1A mRNA and footprinting analysis of its complex with U1A protein. *Biochemistry 36*:1782–1789.

Tsai DE, Keene JD. 1993. In vitro selection of RNA epitopes using autoimmune patient serum. *J Immunol 150*:1137–1145.

Van Venrooij WJ, Hoet R, Castrop J, Hageman B, Mattaj IW, Van De Putte LB. 1990. Anti-(U1) small nuclear RNA antibodies in anti-small nuclear ribonucleoprotein sera from patients with connective tissue diseases. *J Clin Invest 86*:2154–2160.